

Supplemental Materials

A Mathematical Model for Covalent Proteolysis Targeting Chimeras: Thermodynamics and Kinetics underlying Catalytic Efficiency

Charu Chaudhry^{1*}

¹Molecular & Cellular Pharmacology, Lead Discovery, Janssen Research and Development, LLC , Spring House, PA 19477, United States.

*Corresponding Author

Table of Contents

1. Parameter Sensitivity Analysis.....	S2
2. Reaction kinetics.....	S4
3. References.....	S6
4. Chemical Kinetic ODEs	S7
• Core Reversible Model.....	S7
• Covalent E3 Model.....	S9
• Covalent Target Model.....	S11

Supplemental Information

Parameter Sensitivity Analysis

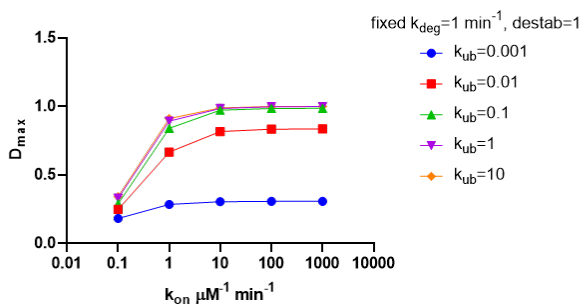
The model captures a range of degradation efficacy using different values of the input parameters. In our simulations, we considered how changes in measurable parameters affected the resultant degradation efficacy. Typically known or measurable parameters include concentration of target, ligase, binary PROTAC affinity to POI and E3 and target half-life. We also identified 3 parameters k_{on} , k_{ub} , k_{deg} that are more difficult to measure having the least amount of direct measurement support, and therefore jointly varied these over several orders of magnitude. In addition, we incorporated into the analysis a 'destab' term, a tunable factor to offset the energetics of the ubiquitinated ternary complex relative to the non-ubiquitinated; a multiplicative factor in ternary on and offrate such that $k_{off_Tub_PL} = destab * k_{on_TP} * K_{TubP} / \alpha$; $k_{off_TubP_L} = destab * k_{on_PL} * K_{PL} / \alpha$. This is supported by the experimental evidence that most stable ternary complexes lead to enhanced ubiquitination and degradation rates, where the overall rate of dissociation of the ubiquitinated protein from the ternary complex is likely to be much faster and not rate limiting¹⁻². While this implies weaker stability of ubiquitinated ternary relative to the non-ubiquitinated ternary, no quantitative experimental data is available. Thus sensitivity analysis was carried out on destab varying it over 10,000 fold, in addition to the afore mentioned 3 parameters. Maximal degradation achieved over a range of concentrations (D_{max}) was computed, and parameter sensitivity of D_{max} was visualized by plotting D_{max} changes with respect to changes in 2 parameters with the other 2 held fixed at their nominal value for each pair of combinations (see Fig S1).

Results demonstrated that most of the outcomes are well determined by parameters we can measure (e.g. affinity to both target and E3 ligase, target and E3 half-life), and that the model can generate a wide range of outcomes with D_{max} trends that are holding over broad parameter ranges for underdetermined parameters. We find that k_{on} , k_{ub} , k_{deg} are sensitive parameters in the model, with most of their sensitivity in the lower parameter value regimes and expected interdependencies to increase or decrease degradation. Maximum degradation is achieved when all the rates are fast, but there are limits on their values such that $k_{on} > 10 \text{ uM}^{-1}\text{min}^{-1}$, $k_{ub} > 0.1 \text{ min}^{-1}$, $k_{deg} > 0.01 \text{ min}^{-1}$ does not lead to further enhancement of degradation; maximum setpoint is determined when all the target is degraded, for the current system parameters.

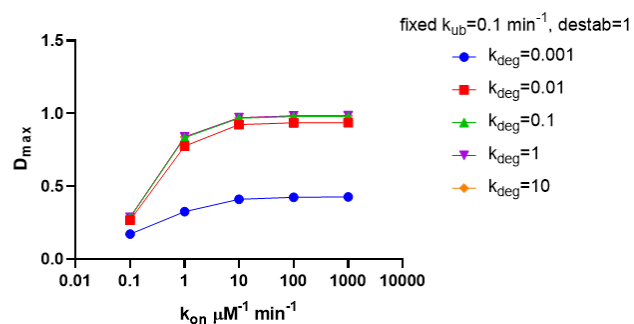
For k_{on} , sensitivity is seen in all regimes expected. For slow k_{on} , not much degradation is observed because complex formation is inefficient. Most of the k_{on} sensitivity is observed at values below $1 \mu\text{M}^{-1}\text{min}^{-1}$. A wide spectrum of degradation is observed at fast k_{on} , driven by the k_{ub} and k_{deg} rates. The model is also sensitive to differences in k_{ub} , which is a PROTAC and ligase dependent parameter. In the case of a non-optimal PROTAC geometry for catalysis, a slow k_{ub} rate of 0.001 min^{-1} significantly reduces degradation efficacy predicted by the model. For efficient ubiquitination, at a rate of 0.1 min^{-1} , the predicted degradation efficacy increases as expected and is also captured by the model. Notably, we are simulating a target with intrinsic half-life of 24 hr ($k_{deg,int} \sim 4.8 \times 10^{-4} \text{ min}^{-1}$), so 0.01 min^{-1} is already at 20x the intrinsic rate, where PROTAC degradation is very efficient and only 5% of target is remaining. Effects of k_{deg} and k_{on} will change based on target half-life (see Fig. 8).

For $destab$ changes over 10,000-fold, the results indicated that target degradation levels were largely insensitive, for the remaining parameters used in the simulation. We hypothesize this is because ubiquitinated ternary complex is never more than a small fraction of the total target such that changes in relative stability of ubiquitinated to non-ubiquitinated ternary do not significantly impact increase in degradation. See Figure S2 comparing ubiquitinated ternary to other species. This can be explored further in future analyses.

A



B



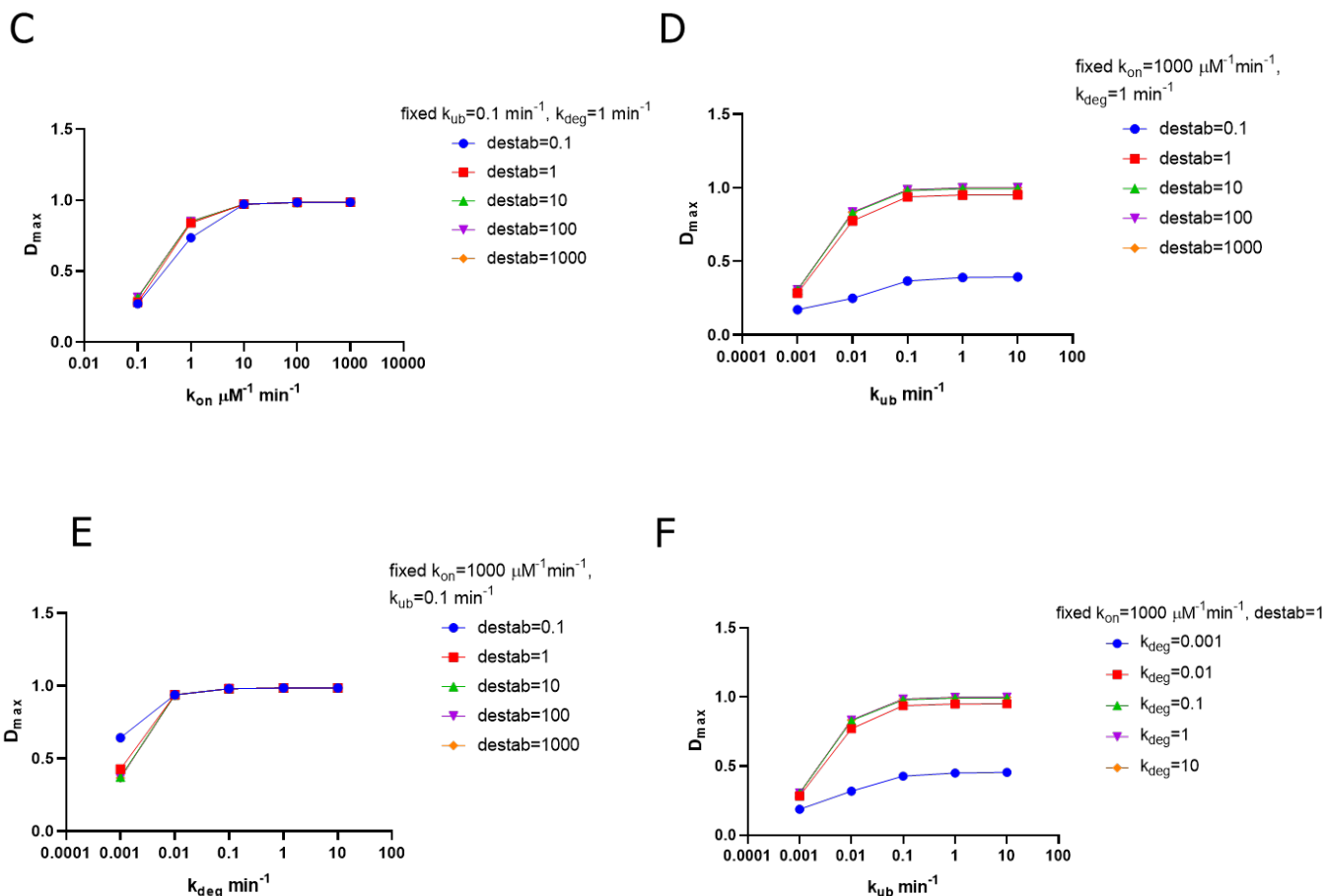


Figure S1. Results of sensitivity analysis plotting D_{max} varying 2 parameters over 10,000 fold while holding 2 others fixed. A. k_{on} and k_{ub} varied at fixed k_{deg} of $1 min^{-1}$ and $destab$ 1, B. k_{on} and k_{deg} varied at fixed $k_{ub}=0.1 min^{-1}$ and $destab$ 1, C. k_{ub} and k_{deg} varied at fixed k_{on} $1000 \mu M^{-1} min^{-1}$ and $destab$ 1, D. k_{ub} and $destab$ at fixed $k_{on}=1000 \mu M^{-1} min^{-1}$ and $k_{deg}=1 min^{-1}$, E. k_{deg} and $destab$ varied at fixed $k_{on}=1000 \mu M^{-1} min^{-1}$ and $k_{ub}=0.1 min^{-1}$, and F. k_{on} and $destab$ varied at fixed $k_{ub}=0.1 min^{-1}$ and $k_{deg}=1 min^{-1}$. Global simulation parameters include $[T]=[L]=0.01 \mu M$, target half-life=24 hr, E3 half-life=24 hr, $K_{TP}=0.01 \mu M$, $K_{PL}=1 \mu M$, $k_{inact}=0.1 min^{-1}$.

Reaction kinetics: covalent bond formation, degradation and PROTAC consumption-

To understand the interplay between the kinetics of covalent bond formation to E3 ligase/POI and degradation, we compared the dynamics of each species in the system (Fig S2). We leveraged these simulations to gain insight into the formation and dissipation of key ternary and ubiquitinated POI in the

reaction, which are more challenging to measure experimentally. Notably, both covalent POI and E3 cases exhibit an initial transient increase in total ternary and ubiquitinated POI with similar temporal profiles and greater magnitude in the covalent E3 case (Fig S2B,C), while for the reversible case the transient for both species is flat (Fig S2A). In the case of a covalent E3 ligase PROTAC, total ternary and ubiquitinated POI both reach a similar steady state and >99% POI degradation is achieved in 3 hours (Supp Fig 2B). In contrast in the covalent POI PROTAC scenario, the disappearance of PROTAC occurs significantly more rapidly, leading to a concomitant rapid loss of ternary and ubiquitinated POI that coincides with recovery in target levels (Fig S2C). This is because PROTAC is consumed in every cycle of target degradation, driving down the available PROTAC concentration remaining in the system. Over the course of the reaction, >99% of covalent POI PROTAC is consumed, in contrast to only ~ 30% of total PROTAC loss due to turnover of the covalent E3 ligase-PROTAC complex under similar conditions.

To test the difference in degradation efficacy between a covalent E3 ligase-PROTAC and a “regenerating” covalent POI-PROTAC, we tested the hypothetical case where a fully functional PROTAC can be regenerated during proteasomal degradation of the POI instead of being irreversibly lost on turnover of the covalent POI-PROTAC complex. This approximates the case of a reversible covalent inhibitor. As shown in the simulation results in Fig S2D, total PROTAC is now no longer consumed during the reaction. Greater depth of degradation is observed for the covalent POI- PROTAC regeneration case versus the original covalent POI PROTAC (compare 2D vs 2C), but this still falls short of the covalent E3 ligase PROTAC (2B) by ~2 fold. We hypothesize that the ~ two-fold enhancement in degradation in the covalent E3 ligase system is due to greater catalytic cycling, underscoring the true catalytic benefit from stabilizing the activated ligase complex. This value will likely be dependent on specific system parameters.

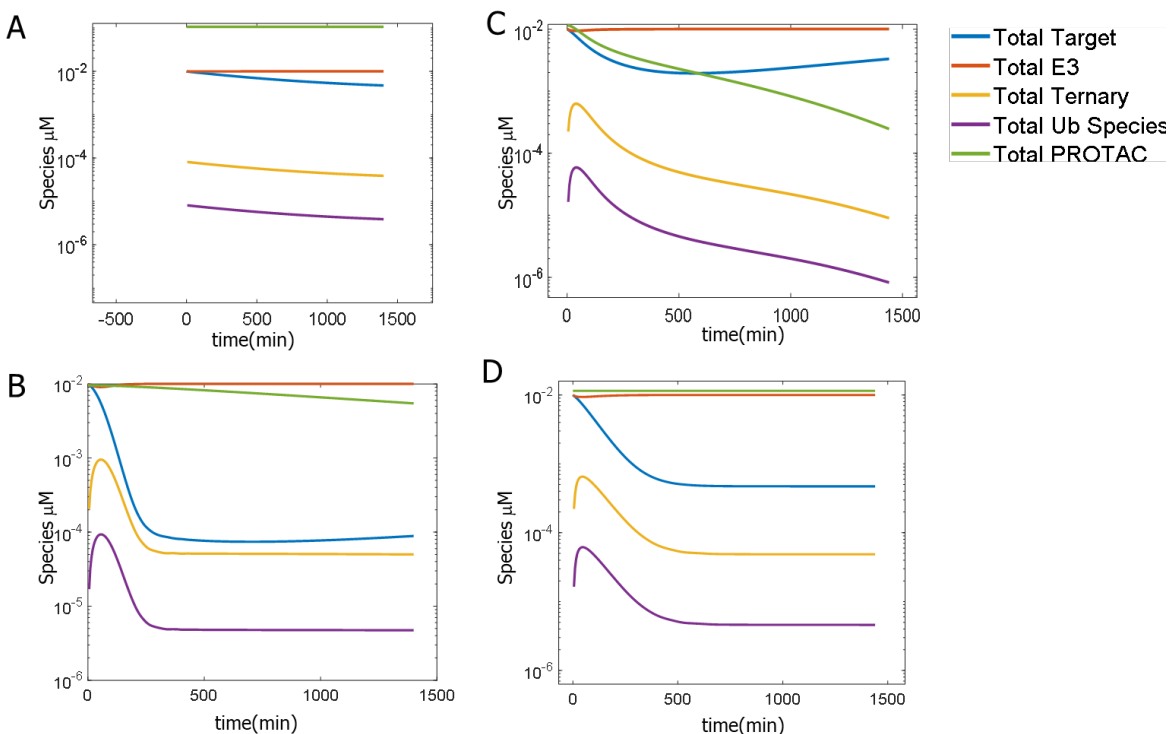


Figure S2. Kinetic simulations of Reversible and Covalent E3 and POI TPD reactions. Time courses following total target, E3 ligase, and key ternary and ubiquitinated POI intermediates are shown under the following conditions: fully reversible (no inactivation); $K_{TP} = 0.01 \mu\text{M}$ $K_{PL} = 1 \mu\text{M}$ (A); covalent E3 binding; $K_{PL} = 1 \mu\text{M}$, $K_{TP} = 0.01 \mu\text{M}$ (B); covalent target binding; $K_{PL} = 0.01 \mu\text{M}$, $K_{TP} = 1 \mu\text{M}$ (C); same as C but allow regeneration of the PROTAC after a single round of target degradation (D). Single [PROTAC] plotted in each kinetic trace representing concentration that yielded maximum ternary complex at $t=0$ under each simulation condition; $0.11 \mu\text{M}$ for A, $0.01 \mu\text{M}$ for B, C, and D. Global simulation parameters include $[T]=[L]=0.01 \mu\text{M}$, target half-life=24 hr, E3 half-life=24 hr, $k_{on}=6000 \mu\text{M}^{-1}\text{min}^{-1}$, $k_{ub}=0.1 \text{min}^{-1}$, $k_{inact}=1 \text{min}^{-1}$, $k_{deg}=1 \text{min}^{-1}$, with binary affinities varying as described above.

References

1. Imaide, S.; Riching, K. M.; Makukhin, N.; Vetma, V.; Whitworth, C.; Hughes, S. J.; Trainor, N.; Mahan, S. D.; Murphy, N.; Cowan, A. D.; Chan, K. H.; Craigon, C.; Testa, A.; Maniaci, C.; Urh, M.; Daniels, D. L.; Ciulli, A., Trivalent PROTACs enhance protein degradation via combined avidity and cooperativity. *Nat Chem Biol* **2021**, *17* (11), 1157-1167.
2. Roy, M. J.; Winkler, S.; Hughes, S. J.; Whitworth, C.; Galant, M.; Farnaby, W.; Rumpel, K.; Ciulli, A., SPR-Measured Dissociation Kinetics of PROTAC Ternary Complexes Influence Target Degradation Rate. *ACS Chem Biol* **2019**, *14* (3), 361-368.

Chemical Kinetic ODEs for Reversible and Covalent PROTACs

1 Core Reversible Model: Binary and Ternary Complex

$$\frac{dT}{dt} = k_{off}^{T-P} * TP + k_{off}^{T-PL} * TPL - (k_{on} * P + k_{on} * PL) * T \quad (1)$$

$$\frac{dP}{dt} = k_{off}^{T-P} * TP + k_{off}^{P-L} * PL - (k_{on} * T + k_{on} * L) * P \quad (2)$$

$$\frac{dL}{dt} = k_{off}^{P-L} * PL + k_{off}^{TP-L} * TPL - (k_{on} * P + k_{on} * TP) * L \quad (3)$$

$$\frac{dTP}{dt} = k_{on} * T * P + k_{off}^{TP-L} * TPL - (k_{off}^{T-P} + k_{on} * L) * TP \quad (4)$$

$$\frac{dPL}{dt} = k_{on} * P * L + k_{off}^{T-PL} * TPL - (k_{off}^{P-L} + k_{on} * T) * PL \quad (5)$$

$$\frac{dTPL}{dt} = k_{on} * TP * L + k_{on} * PL * T - (k_{off}^{T-PL} + k_{off}^{TP-L}) * TPL \quad (6)$$

2 Core Reversible Model: Ubiquitination and Degradation Complex

$$\frac{dT}{dt} = k_{degint} * (T_0 - T) + k_{off}^{T-P} * TP + k_{off}^{T-PL} * TPL - (k_{on} * P + k_{on} * PL) * T \quad (7)$$

$$\frac{dP}{dt} = k_{off}^{T-P} * TP + k_{off}^{P-L} * PL - (k_{on} * T + k_{on} * L) * P + k_{off}^{T_{ub}} * T_{ub}P - k_{on} * T_{ub} * P \quad (8)$$

$$\begin{aligned} \frac{dL}{dt} = & k_{off}^{P-L} * PL + k_{off}^{TP-L} * TPL - (k_{on} * P + k_{on} * TP) * L \\ & + k_{off}^{T_{ub}P-L} * T_{ub}PL - k_{on} * T_{ub}P * L \end{aligned} \quad (9)$$

$$\frac{dTP}{dt} = k_{on} * T * P + k_{off}^{TP-L} * TPL - (k_{off}^{T-P} + k_{on} * L) * TP - k_{degint} * TP \quad (10)$$

$$\begin{aligned} \frac{dPL}{dt} = & k_{on} * P * L + k_{off}^{T-PL} * TPL - (k_{off}^{P-L} + k_{on} * T) * PL \\ & + k_{off}^{T_{ub}-PL} * T_{ub}PL - k_{on} * T_{ub} * PL \end{aligned} \quad (11)$$

$$\frac{dTPL}{dt} = k_{on} * TP * L + k_{on} * PL * T - (k_{off}^{T-PL} + k_{off}^{TP-L} + k_{ub}) * TPL \quad (12)$$

$$\begin{aligned} \frac{dT_{ub}PL}{dt} = & k_{ub} * TPL + k_{on} * T_{ub}P * L + k_{on} * PL * T_{ub} - (k_{off}^{T_{ub}-PL} \\ & + k_{off}^{T_{ub}P-L}) * T_{ub}PL \end{aligned} \quad (13)$$

$$\frac{dT_{ub}P}{dt} = k_{on} * T_{ub} * P + k_{off}^{T_{ub}P-L} * T_{ub}PL - (k_{off}^{T_{ub}-P} + k_{on} * L) * T_{ub}P \quad (14)$$

$$\frac{dT_{ub}}{dt} = k_{off}^{T_{ub}-P} * T_{ub}P + k_{off}^{T_{ub}-PL} * T_{ub}PL - (k_{on} * P + k_{on} * PL + k_{deg}) * T_{ub} \quad (15)$$

$$\frac{dT_{deg}}{dt} = k_{deg} * T_{ub} \quad (16)$$

3 Covalent E3 Model: Binary and Ternary Complex

$$\begin{aligned} \frac{dT}{dt} = & k_{off}^{T-P} * TP + k_{off}^{T-PL} * TPL - (k_{on}^{TP} * P + k_{on}^{TP} * PL) * T \\ & - (k_{on}^{TP} * T) * PL_c + (k_{off}^{T-PL}) * TPL_c \end{aligned} \quad (17)$$

$$\frac{dP}{dt} = k_{off}^{T-P} * TP + k_{off}^{P-L} * PL - (k_{on}^{TP} * T + k_{on}^{PL} * L) * P \quad (18)$$

$$\frac{dL}{dt} = k_{off}^{P-L} * PL + k_{off}^{TP-L} * TPL - (k_{on}^{PL} * P + k_{on}^{TP} * TP) * L \quad (19)$$

$$\frac{dTP}{dt} = k_{on}^{TP} * T * P + k_{off}^{TP-L} * TPL - (k_{off}^{T-P} + k_{on}^{PL} * L) * TP \quad (20)$$

$$\frac{dPL}{dt} = k_{on}^{PL} * P * L + k_{off}^{T-PL} * TPL - (k_{off}^{P-L} + k_{on}^{TP} * T + k_{inact}^{PL}) * PL \quad (21)$$

$$\frac{dTPL}{dt} = k_{on}^{PL} * TP * L + k_{on}^{TP} * PL * T - (k_{off}^{T-PL} + k_{off}^{TP-L}) * TPL - k_{inact}^{PL} * TPL \quad (22)$$

$$\frac{dPL_c}{dt} = k_{inact}^{PL} * PL + k_{off}^{T-PL} * TPL_c - (k_{on}^{TP} * T) * PL_c \quad (23)$$

$$\frac{dTPL_c}{dt} = k_{inact}^{PL} * TPL + k_{on}^{TP} * T * PL_c - (k_{off}^{T-PL}) * TPL_c \quad (24)$$

4 Covalent E3 Model: Ubiquitination and Degradation Complex

$$\begin{aligned} \frac{dT}{dt} = & k_{degint}^T * (T_0 - T) + k_{off}^{T-P} * TP + k_{off}^{T-PL} * (TPL + TPL_c) \\ & - (k_{on}^{TP} * P + k_{on}^{TP} * PL + k_{on}^{TP} * PL_c) * T \end{aligned} \quad (25)$$

$$\begin{aligned} \frac{dP}{dt} = & k_{off}^{T-P} * TP + k_{off}^{P-L} * PL - (k_{on}^{TP} * T + k_{on}^{PL} * L) * P + k_{off}^{Tub-P} * TubP \\ & - k_{on}^{Tub-P} * Tub * P + k_{degint}^L * PL + k_{degint}^T * TP \end{aligned} \quad (26)$$

$$\begin{aligned} \frac{dL}{dt} = & k_{degint}^L * (L_0 - L) + k_{off}^{P-L} * PL + k_{off}^{TP-L} * TPL - (k_{on}^{PL} * P \\ & + k_{on}^{PL} * TP) * L + k_{off}^{Tub^P-L} * TubPL - k_{on}^{PL} * TubP * L \end{aligned} \quad (27)$$

$$\frac{dTP}{dt} = k_{on}^{TP} * T * P + k_{off}^{TP-L} * TPL - (k_{off}^{T-P} + k_{on}^{PL} * L) * TP - k_{degint}^T * TP \quad (28)$$

$$\begin{aligned} \frac{dPL}{dt} = & k_{on}^{PL} * P * L + k_{off}^{T-PL} * TPL - (k_{off}^{P-L} + k_{on}^{TP} * T) * PL \\ & + k_{off}^{Tub-PL} * TubPL - k_{on}^{Tub^P} * Tub * PL - k_{degint}^L * PL - k_{inact}^{PL} * PL \end{aligned} \quad (29)$$

$$\frac{dTPL}{dt} = k_{on}^{PL} * TP * L + k_{on}^{TP} * PL * T - (k_{off}^{T-PL} + k_{off}^{TP-L} + k_{ub} + k_{inact}^{PL}) * TPL \quad (30)$$

$$\begin{aligned} \frac{dTubPL}{dt} = & k_{ub} * TPL + k_{on}^{PL} * TubP * L + k_{on}^{Tub^P} * PL * Tub \\ & - (k_{off}^{Tub-PL} + k_{off}^{Tub^P-L} + k_{inact}^{PL}) * TubPL \end{aligned} \quad (31)$$

$$\frac{dTubP}{dt} = k_{on}^{Tub^P} * Tub * P + k_{off}^{Tub^P-L} * TubPL - (k_{off}^{Tub-P} + k_{on}^{PL} * L) * TubP \quad (32)$$

$$\begin{aligned} \frac{dTub}{dt} = & k_{off}^{Tub-P} * TubP + k_{off}^{Tub-PL} * TubPL - (k_{on}^{Tub^P} * P \\ & + k_{on}^{Tub^P} * PL + k_{on}^{Tub^P} * PL_c + k_{deg}) * Tub + k_{off}^{Tub-PL} * TubPL_c \end{aligned} \quad (33)$$

$$\frac{dTdeg}{dt} = k_{deg} * Tub \quad (34)$$

$$\begin{aligned} \frac{dPL_c}{dt} = & k_{inact}^{PL} * PL + k_{off}^{T-PL} * TPL_c - (k_{on}^{TP} * T) * PL_c \\ & + k_{off}^{Tub-PL} * (TubPL_c) - k_{on}^{Tub^P} * Tub * PL_c - k_{degint}^L * PL_c \end{aligned} \quad (35)$$

$$\frac{dTPL_c}{dt} = k_{inact}^{PL} * TPL + k_{on}^{TP} * T * PL_c - (k_{off}^{T-PL} + k_{ub}) * TPL_c \quad (36)$$

$$\frac{dTubPL_c}{dt} = k_{inact}^{PL} * TubPL + k_{ub} * TPL_c + k_{on}^{Tub^P} * Tub * PL_c - (k_{off}^{Tub-PL}) * TubPL_c \quad (37)$$

5 Covalent Target Model: Binary and Ternary Complex

$$\frac{dT}{dt} = k_{off}^{T-P} * TP + k_{off}^{T-PL} * TPL - (k_{on}^{TP} * P + k_{on}^{TP} * PL) * T \quad (38)$$

$$\frac{dP}{dt} = k_{off}^{T-P} * TP + k_{off}^{P-L} * PL - (k_{on}^{TP} * T + k_{on}^{PL} * L) * P \quad (39)$$

$$\begin{aligned} \frac{dL}{dt} = & k_{off}^{P-L} * PL + k_{off}^{TP-L} * TPL - (k_{on}^{PL} * P + k_{on}^{PL} * TP) * L \\ & + k_{off}^{TP-L} * T_cPL - (k_{on}^{PL} * L) * T_cP \end{aligned} \quad (40)$$

$$\frac{dTTP}{dt} = k_{on}^{TP} * T * P + k_{off}^{TP-L} * TPL - (k_{off}^{T-P} + k_{on}^{PL} * L + k_{inact}^{TP}) * TP \quad (41)$$

$$\frac{dTPL}{dt} = k_{on}^{PL} * P * L + k_{off}^{T-PL} * TPL - (k_{off}^{P-L} + k_{on}^{TP} * T) * PL \quad (42)$$

$$\frac{dTTPPL}{dt} = k_{on}^{PL} * TP * L + k_{on}^{TP} * PL * T - (k_{off}^{T-PL} + k_{off}^{TP-L}) * TPL - k_{inact}^{TP} * TPL \quad (43)$$

$$\frac{dT_cP}{dt} = k_{inact}^{TP} * TP + k_{off}^{TP-L} * T_cPL - (k_{on}^{PL} * L) * T_cP \quad (44)$$

$$\frac{dT_cPL}{dt} = k_{inact}^{TP} * TPL + k_{on}^{PL} * T_cP * L - (k_{off}^{TP-L}) * T_cPL \quad (45)$$

6 Covalent Target Model: Ubiquitination and Degradation Complex

$$\frac{dT}{dt} = k_{degint}^T * (T_0 - T) + k_{off}^{T-P} * TP + k_{off}^{T-PL} * TPL - (k_{on}^{TP} * P + k_{on}^{TP} * PL) * T \quad (46)$$

$$\begin{aligned} \frac{dP}{dt} = & k_{off}^{T-P} * TP + k_{off}^{P-L} * PL - (k_{on}^{TP} * T + k_{on}^{PL} * L) * P + k_{off}^{T_{ub}-P} * T_{ub}P \\ & - k_{on}^{T_{ub}P} * T_{ub} * P + k_{degint}^T * TP + k_{degint}^L * PL \\ & + \text{switch_regenerate} * (k_{deg} * T_{c_ub}P + k_{degint}^T * T_cP) \end{aligned} \quad (47)$$

$$\begin{aligned} \frac{dL}{dt} = & k_{degint}^L * (L_0 - L) + k_{off}^{P-L} * PL + k_{off}^{TP-L} * TPL - (k_{on}^{PL} * P + k_{on}^{PL} * TP) * L \\ & + k_{off}^{T_{ub}P-L} * T_{ub}PL - k_{on}^{PL} * T_{ub}P * L + k_{off}^{TP-L} * T_cPL + k_{off}^{T_{ub}P-L} * T_{c_{ub}}PL \\ & - k_{on}^{PL} * T_cP * L - k_{on}^{PL} * T_{c_{ub}}P * L \end{aligned} \quad (48)$$

$$\begin{aligned} \frac{dTP}{dt} = & k_{on}^{TP} * T * P + k_{off}^{TP-L} * TPL - (k_{off}^{T-P} + k_{on}^{PL} * L) * TP - k_{degint}^T * TP \\ & - k_{inact}^{TP} * TP \end{aligned} \quad (49)$$

$$\begin{aligned} \frac{dPL}{dt} = & k_{on}^{PL} * P * L + k_{off}^{T-PL} * TPL - (k_{off}^{P-L} + k_{on}^{TP} * T) * PL + k_{off}^{T_{ub}P-L} * T_{ub}PL \\ & - k_{on}^{T_{ub}P} * T_{ub} * PL - k_{degint}^L * PL \end{aligned} \quad (50)$$

$$\frac{dTPL}{dt} = k_{on}^{PL} * TP * L + k_{on}^{TP} * PL * T - (k_{off}^{T-PL} + k_{off}^{TP-L} + k_{ub} + k_{inact}^{TP}) * TPL \quad (51)$$

$$\begin{aligned} \frac{dT_{ub}PL}{dt} = & k_{ub} * TPL + k_{on}^{PL} * T_{ub}P * L + k_{on}^{T_{ub}P} * PL * T_{ub} \\ & - (k_{off}^{T_{ub}P-L} + k_{off}^{T_{ub}P-L} + k_{inact}^{TP}) * T_{ub}PL \end{aligned} \quad (52)$$

$$\begin{aligned} \frac{dT_{ub}P}{dt} = & k_{on}^{T_{ub}P} * T_{ub} * P + k_{off}^{T_{ub}P-L} * T_{ub}PL - (k_{off}^{T_{ub}P} + k_{on}^{PL} * L) * T_{ub}P \\ & - k_{inact}^{TP} * T_{ub}P \end{aligned} \quad (53)$$

$$\frac{dT_{ub}}{dt} = k_{off}^{T_{ub}P} * T_{ub}P + k_{off}^{T_{ub}P-L} * T_{ub}PL - (k_{on}^{T_{ub}P} * P + k_{on}^{T_{ub}P} * PL + k_{deg}) * T_{ub} \quad (54)$$

$$\frac{dT_{deg}}{dt} = k_{deg} * (T_{ub} + T_{c_{ub}}P) \quad (55)$$

$$\frac{dT_cP}{dt} = k_{inact}^{TP} * TP + k_{off}^{TP-L} * T_cPL - (k_{on}^{PL} * L) * T_cP - k_{degint}^T * T_cP \quad (56)$$

$$\frac{dT_cPL}{dt} = k_{inact}^{TP} * TPL + k_{on}^{PL} * T_cP * L - (k_{off}^{TP-L} + k_{ub}) * T_cPL \quad (57)$$

$$\frac{dT_{c_{ub}}PL}{dt} = k_{inact}^{TP} * T_{ub}PL + k_{ub} * T_cPL - k_{off}^{T_{ub}P-L} * T_{c_{ub}}PL + k_{on}^{PL} * T_{c_{ub}}P * L \quad (58)$$

$$\frac{dT_{c_{ub}}P}{dt} = k_{inact}^{TP} * T_{ub}P + k_{off}^{T_{ub}P-L} * T_{c_{ub}}PL - T_{c_{ub}}P * k_{deg} - k_{on}^{PL} * T_{c_{ub}}P * L \quad (59)$$